NJC

Accepted Manuscript

This is an *Accepted Manuscript*, which has been through the Royal Society of Chemistry peer review process and has been accepted for publication.

Accepted Manuscripts are published online shortly after acceptance, before technical editing, formatting and proof reading. Using this free service, authors can make their results available to the community, in citable form, before we publish the edited article. We will replace this *Accepted Manuscript* with the edited and formatted *Advance Article* as soon as it is available.

You can find more information about *Accepted Manuscripts* in the Information for Authors.

Please note that technical editing may introduce minor changes to the text and/or graphics, which may alter content. The journal's standard Terms & Conditions and the Ethical guidelines still apply. In no event shall the Royal Society of Chemistry be held responsible for any errors or omissions in this *Accepted Manuscript* or any consequences arising from the use of any information it contains.

ROYAL SOCIETY OF CHEMISTRY

www.rsc.org/njc

New Journal of Chemistry

ARTICLE

Inclusion complexes of propiconazole nitrate with substituted β-cyclodextrins. Synthesis, *in silico* and *in vitro* assessment of antifungal properties.

Received 11th July 2015,
Accepted 00th November 2015

DOI: 10.1039/x0xx00000x

www.rsc.org/

B. Minea[a, b], N. Marangoci[a], D. Peptanariu[a], I. Rosca[a], V. Nastasa[c], A. Corciova[b], C. Varganici[a], A. Nicolescu[a], A. Fifere[a], A. Neamtu[b], M. Mares[c], M. Barboiu[d, *], M. Pinteala[1, **]

Abstract. Inclusion complexes of protonated propiconazole nitrate (PCZH-NO_3) with three substituted cyclodextrin (CD) derivatives, namely sulfobutylether-β-CD (SBE7-β-CD), sulfated-β-CD (β-CD-SNa) and monochlorotriazinyl-β-CD (MCT-β-CD) were investigated as new antifungal systems and compared with a previously published complex of PCZH-NO_3 with unsubstituted β-CD. The inclusion complexes were prepared by the freeze-drying method and were characterized by ^{1}H-NMR, 2D Roesy NMR and DSC. This study demonstrates the coexistence of two types of PCZH-NO_3 inclusion into the CD cavity. The complexes with SBE7-β-CD had the highest association constant values. Inclusion efficiency was close to 100%. Comparative *in silico* docking and molecular dynamics simulations were performed. The antifungal activity was assessed on *Candida* spp. and was similar for all four inclusion complexes. The cytotoxicity assessed on normal human dermal fibroblasts (NHDF) was significantly higher for the complex with β-CD than that of the complexes of substituted CDs.

Introduction

Fungal infections are an important health issue fuelled, paradoxically, by the advancements in medical care. The great majority of clinically relevant fungi are opportunistic pathogens, that is, they are part of the normal human microbiota, but they can cause infections if the defence mechanisms of the host become in some way impaired. That is the case with patients that receive immunosuppressive therapy, broad spectrum antibiotics, chemotherapy, patients with diabetes or HIV infection, etc. [1]. The fourth source of bloodstream infections as prevalence, *Candida* yeasts are the most frequent fungal pathogen in humans [2], with *C. albicans* as the dominant species, and can reach mortality rates of 50% [1]. The prophylactic administration of antifungals to an increasing population of patients generates antifungal resistance by creating a selective pressure, which favours those non-*albicans Candida* species that are naturally less susceptible to the drugs, such as *C. glabrata*, or strains with acquired resistance-inducing mutations [3,4]. The increasing rates of resistance underline the need for new antifungal agents.

Azoles, diazoles (imidazoles) and triazoles, are the largest and most widely used class of antifungal agents. Because of their toxicity, imidazoles are restricted to topical use, while triazoles are most often used for systemic treatments. Azoles inhibit ergosterol biosynthesis by blocking a key enzyme, lanosterol-14α-demethylase (Erg11p or Cyp51p), through the binding with the heme iron from the active site of the enzyme. The lack of ergosterol primarily damages the plasma membrane and also, indirectly, the cell wall [5–8].

Propiconazole is a triazole developed and marketed by Janssen Pharmaceutics (Belgium) as an antifungal pesticide. Protonated propiconazole nitrate (PCZH-NO_3, Fig. 1), a derivative of propiconazole, was proved to have a better antifungal activity and lower acute toxicity, comparable to those of commercial azole drugs [9,10], which makes it a good candidate for clinical use. As most clinical azoles (with fluconazole as the sole exception), PCZH-NO_3 has the major inconvenient of being hydrophobic, which severely reduces its bioavailability. To address this issue, the formation of a host-guest inclusion complex with β-cyclodextrin (β-CD) as a host carrier molecule was investigated, with good results [10,11]. The parental β-CD was proved to be virtually non-toxic in oral administration and is, therefore, the molecule of choice for

[a] *Centre of Advanced Research in Bionanoconjugates and Biopolymers (IntelCentru) "Petru Poni" Institute of Macromolecular Chemistry, 41A Grigore Ghica Voda Alley, 700487 Iasi, Romania*
[b] *"Gr. T. Popa" University of Medicine and Pharmacy, 16 University Street, 700115 Iasi, Romania*
[c] *Laboratory of Antimicrobial Chemotherapy, "Ion Ionescu de la Brad" University, 8 Sadoveanu Alley, 700489 Iasi, Romania*
[d] *Adaptative Supramolecular Nanosystems Group, Institut Européen des Membranes, ENSCM/UMII/UMR-CNRS 5635, 34095 Montpellier, Cedex 5, France*
* Dr. Mihail Barboiu E-Mail: mihail-dumitru.barboiu@univmontp2.fr; Dr. Mariana Pinteala, E-Mail: pinteala@icmpp.ro
Electronic Supplementary Information (ESI) available: [Computational Studies: SI-1 PCZH-NO_3 – sugar ring center of mass (COM) distances; SI-2 Molecular dynamics snapshots of the PCZH-NO_3 complexes].

this delivery route due to its availability, ease of production and low cost [12]. It has, however, some major shortcomings which render it improper for parenteral delivery. Owing to the strong intramolecular H-bonds, β-CD has a relatively low water solubility of only 18.5 g/L [12,13]. Moreover, it disrupts the membrane by forming inclusion complexes with cholesterol and other membrane components, which translates into one of the highest haemolytic activity of all cyclodextrins commonly used in pharmaceutics and high nephrotoxicity [13,14]. A solution to these problems is to replace the parental β-CD with derivatives resulted from the partial substitution of its hydroxyl groups with various other chemical moieties. Depending on the nature of the substituent, this can reduce crystallinity, which increases solubility, and can also lower the toxicity [12].

Three such derivatives were selected for this study (Fig. 1), all with higher aqueous solubility and low toxicity. Sulfobutylether-β-cyclodextrin (SBE7-β-CD, Captisol®) is a β-CD derivative statistically substituted at the 2, 3, and 6 positions of the glucopyranose units, with an average degree of substitution of approximately seven. The substituent consists of a sodium sulfonate salt separated from the hydrophobic cavity by a butyl ether spacer group. It has a high solubility in water of more than 700 g/L [15] and is virtually non-toxic [16]. In addition, the substituents improve complexation by extending the original hydrophobic cavity [17]. For comparison, sulfated-β-CD (β-CD-SNa), a derivative with similar aqueous solubility and low toxicity [18], was also tested. In this case the substituent consists of the same sodium sulfonate salt directly linked to the hydroxylic oxygen of the pyranose unit, without the butyl ether spacer. We presumed that the anionic charge given by the sulfate groups would favour the inclusion of cationic protonated propiconazole. Finally, monochlorotriazinyl-β-CD (MCT-β-CD), a neutral cyclodextrin with an average degree of substitution of 0.4 per pyranose unit [19], was investigated. It was also proven to be non-toxic and have a high solubility in water [20]. Moreover, the triazinyl substituent may have antimicrobial activity itself [21].

To the best of our knowledge, this is the first study to report the synthesis and characterisation of the inclusion complexes formed by PCZH-NO_3 with SBE7-β-CD, β-CD-SNa and MCT-β-CD. For comparison, the inclusion complex between PCZH-NO_3 and the parental β-CD was used as a model. The inclusion complexes were prepared using the freeze-drying method. The structures were confirmed by nuclear magnetic resonance spectroscopy (^{1}H-NMR), differential scanning calorimetry (DSC) and *in silico* docking and molecular dynamics simulations. To determine the biological relevance, the antifungal activity and cytotoxicity of their complexes with PCZH-NO_3 were assessed and compared to those of the complex with the parental β-CD.

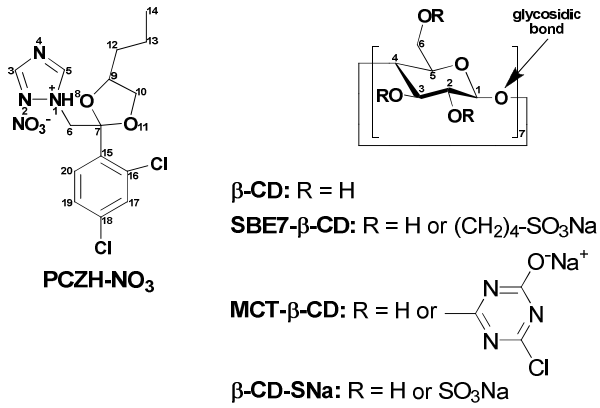

Figure 1. The chemical structures of PCZH-NO_3, β-CD and its derivatives used in this study.

Experimental

Materials

Sulfobutylether-β-cyclodextrin sodium salt (SBE7-β-CD, Captisol®) was purchased from Ligand Pharmaceuticals, Inc.; monochlorotriazinyl-β-cyclodextrin (MCT-β-CD, CAVASOL W7 MCT) was purchased from Wacker Chemie AG; β-Cyclodextrin (β-CD) and β-Cyclodextrin sulfated Na+ salt (β-CD-SNa) were purchased from Sigma–Aldrich; protonated propiconazole nitrate (PCZH-NO_3) was prepared by the treatment of propiconazole (PCZ) with a mixture of nitric and acetic acid in a 1:3 molar ratio in chloroform, at room temperature for 18 h [10]. DMSO-d_6 (99.90% D) and D_2O (98% D) were purchased from Euriso-top. Double distilled water was used throughout the study.

Preparation of inclusion complexes

Inclusion complexes of β-CD, SBE7-β-CD, MCT-β-CD, β-CD-SNa with PCZH-NO_3 were prepared by freeze-drying [10]. In a typical experiment: in 25 mL solution of 1/1 v/v water/methanol 4.349×10^{-4} mol PCZH-NO_3 and 4.349×10^{-4} mol β-CD were added. The resulted solution was maintained under stirring at room temperature for 12 h. The solution was frozen by immersing it in liquid nitrogen and freeze-dried in a Martin Christ, ALPHA 1-2LD Freeze-Dryer for 72 h.

NMR – Nuclear Magnetic Resonance Studies

The NMR spectra were recorded on a Bruker Avance III spectrometer operating at 400.1 MHz for ^{1}H. For the NMR analysis, a 5 mm multinuclear inverse detection z-gradient probe was used. ^{1}H-NMR spectra and H,H ROESY spectra were recorded using standard pulse sequences, as delivered by Bruker, with TopSpin 2.1 PL6 spectrometer control and processing software. The samples were dissolved in either a mixture of DMSO-d_6:D_2O (50:50), in which the solubility of the complexes was very good, or phosphate buffered D_2O (Na_2HPO_4; pH = 7). For all the analyzed solutions the final pH

was around 6.0. Buffer use was necessary to prevent the pH-dependence of the chemical shifts. The proton chemical shifts were reported in ppm, relative to the DMSO-d_6 residual peak (2.512 ppm). For the phosphate buffered D_2O solutions, acetonitril-d_3 was used as internal standard (1.94 ppm).

Computational methods

Docking simulations. As it contains two chiral centers, PCZH-NO_3 is a mixture of four enantiomers [22]. For this study, only one enantiomer (2R, 4S) was chosen for the computational means. To evaluate the association constant (K_a) and the most probable inclusion geometries for SBE7-β-CD/PCZH-NO_3 complexes, molecular docking experiments were performed using AutoDock 4.2 software [23]. For method validation the same calculations were also performed on complexes with β-CD, for which the experimental values were previously determined [10].

The partial atomic charges of the PCZH-NO_3 molecule, used in all molecular docking or molecular dynamics simulations, were derived from *ab initio* calculations at HF/6-31G(d) level using the parallel version of GAMESS-US (ver. R1-2014) [24] and the R.E.D. III Tools suite [25]. The restrained electrostatic potential (RESP) [26] was used to fit the quantum molecular electrostatic potential, with point charges placed at the atomic nuclei. RESP calculations were conducted on the four lowest energy conformations of PCZH-NO_3 obtained in a prior conformational search.

The fitting procedure includes two stages with different weighting factors (0.0005/0.001) and the Connolly surface algorithm, a procedure similar to the one used for Generalized Amber Force Field (GAFF) development [27]. Partial charges for β-CD were taken from q4-MD [28], an optimized version for cyclodextrins of the Glycam 04 force field [29]. For SBE7-β-CD the charge derivation procedure started with the original β-CD charges. To derive the charges on the substitution group, a model molecule of the substituted radical of SBE7-β-CD, namely methyl-1-butyl sulfonate ether (CH_3-O-CH_2-CH_2-CH_2-CH_2-SO_3^-) was used, in a manner similar to that applied for PCZH-NO_3 and described above. Prior to sulfobutyl attachment to β-CD, the methoxy radical (–O–CH_3) on a model molecule was removed and the charge of the carbon bonded to the hydroxilic oxygen of the glucopyranose units (Fig. 1) was adjusted, to give an integer charge of the whole substituted cyclodextrin [30].

The rigid-flexible docking simulations used the hybrid Lamarckian genetic algorithm [31] with 200 runs. CD molecules were considered rigid while PCZH-NO_3 was considered flexible, with 5 freely rotatable bonds. Calculated interaction maps were centred on the CD molecules, with an extension of 30 Å in the x, y and z directions and with a grid spacing of 0.375 Å.

Seven glucopyranose units were substituted with sulfobutyl ether, namely four in position C2 on the secodary rim (residues 1, 3, 5 and 7) and three in position C6 on the primary rim (residues 2, 4 and 6). This assures a sufficient representation of the hindrance induced by the sulfobutyl groups [32].

Molecular dynamics simulations. Molecular dynamics simulations of the CD/PCZH-NO_3 complexes were performed in water in the NPT ensemble (constant number of particles, pressure and temperature). PCZH-NO_3 was modelled by the GAFF force field and for β-CD and SBE7-β-CD description the q4-MD [28] was selected with the charges computed as described above. For water, the TIP3P model [33] was used.

After an initial geometry optimization of each system, 50 ns production runs were performed and used for analysis. For the pressure, the Parrinello-Rahman [34] scheme was used, with a compressibility of 4.5×10^{-5} (bar^{-1}), a relaxation time of 4 ps and a reference pressure of 1 atm. Nosé-Hoover scheme [35,36] was used for temperature coupling at 20°C, with a relaxation constant of 0.5 ps. The electrostatic interactions were evaluated using the particle mesh Ewald (PME) [37] summation method. The molecular dynamics calculations were performed using the GROMACS 4.6.7 suite [38] on GPU equipped servers.

DSC Studies

Differential scanning calorimetry (DSC) measurements were conducted on a DSC 200 F3 Maia device (Netzsch, Germany). Five mg of each sample were heated in aluminium crucibles with pierced and pressed lids. A heating rate of 10°C min^{-1} was applied and nitrogen atmosphere was used as purge gas, at a flow rate of 50 mL min^{-1}. The device was calibrated with indium, according to standard procedures.

In vitro dissolution studies

In vitro dissolution studies of inclusion complexes were performed in triplicate, according to the European Pharmacopoeia, 8th edition [39], using a two-paddle Erweka dissolution tester. For the dissolution tests, 200 mg of PCZH-NO_3 and quantities of the inclusion complexes containing an equivalent amount of triazole were used. The experiments were conducted in physiological conditions, at 37 ± 0.5°C, using 900 mL of phosphate buffer (pH=6.8), with a stirring speed of 100 rpm. At preset time intervals (10, 20, 30, 40, 60, 90 and 120 minutes), 5 mL aliquots were collected (and replaced with equal volumes of fresh medium), filtered through a 0.45 µm filter and analyzed with a UV-VIS spectrophotometer (Jasco V530). The PCZH-NO_3 concentration was determined by a standard method [10].

Biological tests

The antifungal activity of the complexes was assessed on 20 *Candida* spp. clinical isolates (10 *C. albicans* + 10 *C. glabrata*) growing as planktonic phase. The *in vitro* susceptibility testing was performed following the EUCAST EDef 7.2 guidelines [40]. The stock solutions were prepared using DMSO as a solvent. The concentration range of the tested antifungals was 0.0156 - 8 mg/L (concentration of the active principle). The minimum inhibitory concentrations (MICs) were determined spectrophotometrically at 405 nm, after 24h of incubation at 35°C, using an iMark Microplate Reader (Bio-rad Laboratories,

USA). A 50% reduction in growth (compared with the drug free well) was used as MIC endpoint for all tested complexes.

To assess the cytotoxicity, the CellTiter 96® AQueous One Solution Cell Proliferation Assay (Promega) was performed on normal human dermal fibroblasts - NHDF (PromoCell) by following the protocol recommended by the manufacturer [41]. The cells were grown in DMEM:F12 medium (Lonza) supplemented with 10% fetal bovine serum (Gibco), 1mM sodium pyruvate (Lonza) and 1% Penicillin-Streptomycin-Amphotericin B mixture (10K/10K/25 µg in 100 mL, Lonza). The same medium was used to prepare serial dilutions of the compounds to be tested.

To ensure cell adhesion, NDHF were seeded at 5×10^3 cells/well in 96-well tissue culture plates and incubated for 24 h at 37°C under humidified atmosphere with 5% CO_2. The medium was then replaced with 100 µL/well of the previously prepared dilutions and plates were further incubated for 20 h. The CellTiter 96® AQueousOne Solution reagent was then added to each well and, after a final four hour incubation, the absorbance at 490 nm was recorded with an EnVision® plate reader (PerkinElmer).

Statistical analysis

GraphPad Prism 6.04 for Windows (GraphPad Software, La Jolla California USA, www.graphpad.com) was used for data analysis. The one-way ANOVA for repeated measures, with the Greenhouse-Geisser correction, and Tukey's multiple comparisons test were used to compare the antifungal activities of the four complexes. Differences were considered significant at two-tailed $P<0.05$. To calculate the half maximal inhibitory concentrations (IC_{50}), a log(inhibitor) vs. response with variable slope (four parameters) nonlinear regression model was used.

Results & discussion

Synthesis

The inclusion complexes of different cyclodextrins with PCZH-NO_3 were prepared by freeze-drying, using 1/1 v/v water/methanol solutions of β-CD [10], SBE7-β-CD, MCT-β-CD, β-CD-SNa, and PCZH-NO_3 in a 1/1 molar ratio. Inclusion complexes presented in the form of white powder, with yields close to 100% as demonstrated by DSC studies (Section 3.3).

NMR experiments

The complex formation is usually followed trough variations in some proton chemical shifts of guest and host molecules. When the inclusion complex is formed, the cyclodextrin inner protons (H-3 and H-5, Fig. 1) suffer an up-field shift due to the magnetic anisotropy effects produced by the guest molecule. Unlike β-CD (used as a model), the three CD derivatives can be considered as a statistical mixtures of different stereoisomers, due to their chemical modifications. As a consequence, they have unresolved broad peaks, especially β-CD-SNa and SBE7-β-CD, making difficult, even impossible, to follow the chemical shifts of their H-3 and H-5 protons. Therefore, the formation of the inclusion complexes was deduced from the chemical shift changes of PCZH-NO3 aromatic protons. In the ^{1}H-NMR spectrum (Fig. 2-4), the signals corresponding to two diastereoisomers [10,22] were in a ratio of 1:2, as determined from the integral values. ^{1}H-NMR spectra of the inclusion complexes showed changes in resonance frequencies for the aromatic protons of both triazole (H-3 and H-5) and 2,4-diclorophenyl (H-17, H-19 and H-20) group. The chemical shifts differences are summarized in Table 1. Moreover, the appearance of additional signals in the ^{1}H-NMR spectrum of SBE7-β-CD/PCZH-NO_3 inclusion complex in (Fig. 3) can be attributed to the chiral selector properties of the cyclodextrin.

The association constants (K_a) of the inclusion complexes were determined by ^{1}H-NMR titration of protonated propiconazole nitrate with each cyclodextrin by using the chemical shifts of the 2,4-dichlorophenyl protons and by applying the NMR version of the Benesi-Hildebrand equation (1) [42]:

$$\frac{1}{\Delta\delta} = \frac{1}{K_a \Delta\delta_{max}[H]_0} + \frac{1}{\Delta\delta_{max}} \quad (1)$$

Where, Δδ is the observed chemical shift difference of the guest for a given cyclodextrin concentration ($[H]_0$) and $\Delta\delta_{max}$ is the chemical shift difference between a pure sample of complex and the free guest.

The ^{1}H-NMR spectra of different mixtures of PCZH-NO_3 and cyclodextrins were recorded by keeping the concentration of PCZH-NO_3 constant and varying the concentrations of the cyclodextrins. The double-reciprocal plots of the NMR version of the Benesi-Hildebrand equation (Fig. 5) gave straight lines, confirming the 1:1 stoichiometry of the inclusion complexes [43]. The values of the association constants were 510, 1050 and 250 M^{-1} for β-CD, SBE7-β-CD and MCT-β-CD, respectively.

We have to mention that the chemical shifts of the triazolic ring can induce experimental errors in describing the cyclodextrin-drug interactions, because these shifts depend not only on the interactions with the modified cyclodextrins but also they are sensitive to many other physical and chemical parameters, such as solvent, pH, concentration, purity, temperature, etc. [44,45]. Consequently, the variation of the ^{1}H-NMR chemical shifts of the triazolic ring cannot be taken into consideration for determining association constants with cyclodextrins.

The association constant of the β-CD-SNa/PCZH-NO_3 inclusion complex cannot be determined since the variation of the chemical shifts of the dichlorophenyl protons did not follow a linear trend, possibly due to the high concentration of the anionic groups close to the CD rim, which can induce perturbations on the chemical shifts of the PCZH-NO_3 protons.

The formation of the inclusion complexes was further confirmed from ROESY (rotating frame Overhauser effect spectroscopy) experiments (Fig. 6). In this type of experiment inter- and intramolecular interactions can be observed. If two protons from different compounds are in spatial vicinity within 3-5 Å, a NOE cross-peak is observed in 2D ROESY spectrum.

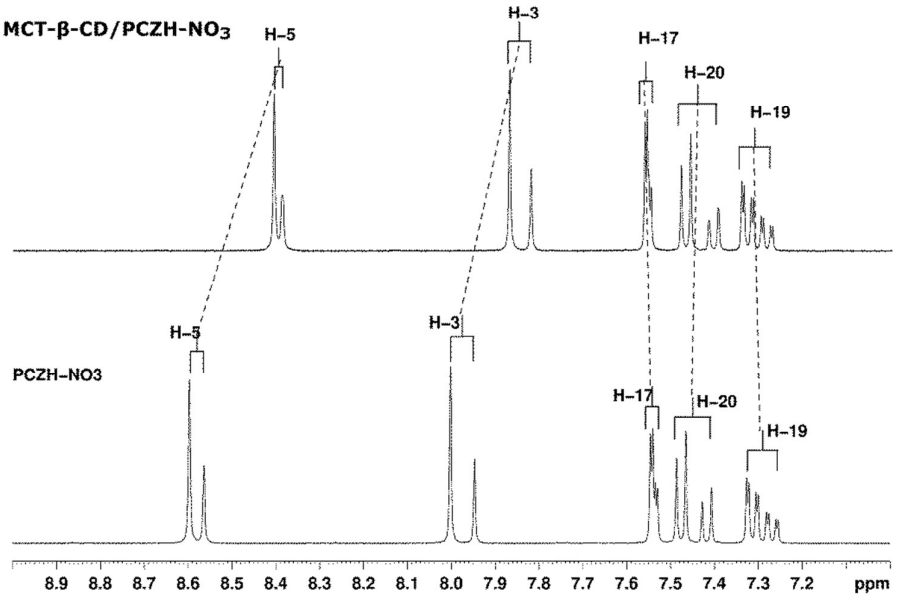

Figure 2. ^{1}H-NMR spectra of PCZH-NO_3 and MCT-β-CD/PCZH-NO_3 inclusion complex, recorded in DMSO-d_6:D_2O mixture

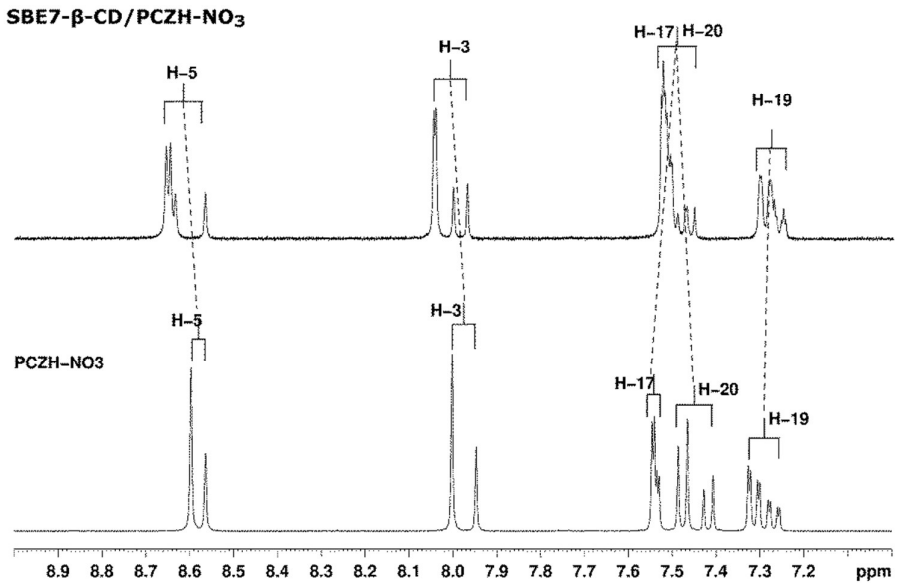

Figure 3. ^{1}H-NMR spectra of PCZH-NO_3 and SBE7-β-CD/PCZH-NO_3 inclusion complex, recorded in DMSO-d_6:D_2O mixture.

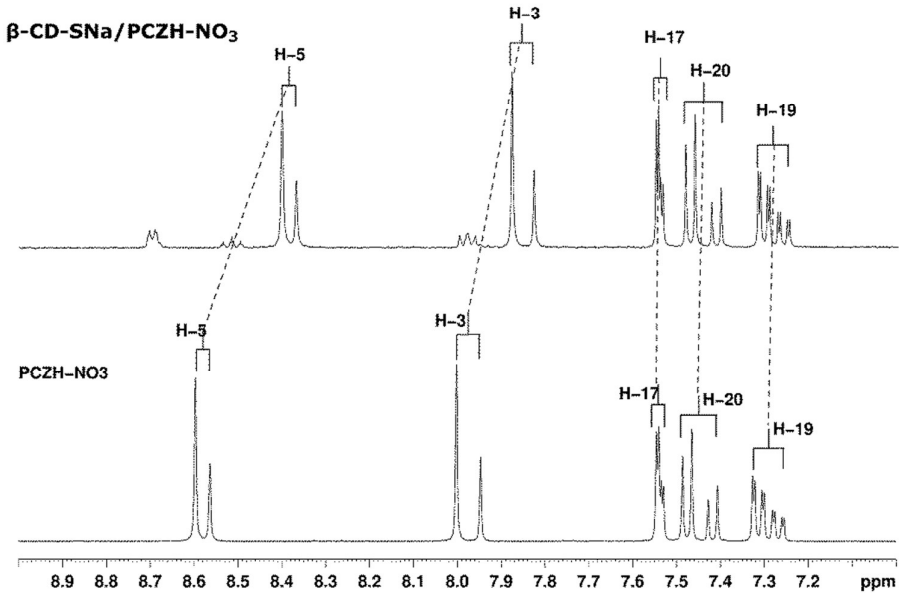

Figure 4. ^{1}H-NMR spectra of PCZH-NO_3 and β-CD-SNa/PCZH-NO_3 inclusion complex, recorded in DMSO-d_6:D_2O mixture.

Table 1. Changes in the chemical shifts of PCZH-NO_3 aromatic protons in the presence of the studied cyclodextrins (m* multiplicity).

Proton label	PCZH-NO_3		β-CD-SNa/PCZH-NO_3		MCT-β-CD/PCZH-NO_3		SBE7-β-CD/PCZH-NO_3	
	Major isomer δ ppm (m*)	Minor isomer δ ppm (m*)	Major isomer δ ppm	Minor isomer δ ppm	Major isomer δ ppm	Minor isomer δ ppm	Major isomer δ ppm	Minor isomer δ ppm
H-5	8.5985(s)	8.5653(s)	8.4018 Δ= -0.1967	8.3694 Δ=-0.1959	8.4083 Δ=0.1902	8.3904 Δ=-0.1749	8.6571 Δ=0.0586 8.6474 Δ=0.049	8.6360 Δ=0.0707 8.5680 Δ=0.0027
H-3	8.0033(s)	7.9484(s)	7.8785 Δ= -0.1248	7.8285 Δ=-0.1199	7.8723 Δ=-0.131	7.8236 Δ=-0.1248	8.0479 Δ=0.0446 8.0435 Δ=0.0402	8.0034 Δ=0.055 7.9718 Δ=0.0234
H-17	7.5447(d)	7.534(d)	7.548 Δ= 0.0033	7.5381 Δ=0.0041	7.5624 Δ=0.0177	7.5537 Δ=0.0197	7.5285 Δ=-0.0162 7.5204 Δ=-0.0243	7.5085 Δ=-0.0255
H-20	7.4773(d)	7.4188(d)	7.4728 Δ= -0.0045	7.4135 Δ=-0.0053	7.4715 Δ=-0.0058	7.4084 Δ=-0.0104	7.5182 Δ=-0.041	7.4846 Δ=0.0658 7.4636 Δ=0.045
H-19	7.3176(dd)	7.2724(dd)	7.3083 Δ= -0.0093	7.2632 Δ=-0.0092	7.3341 Δ=0.0165	7.2901 Δ=0.0177	7.2930 Δ=-0.0246	7.2633 Δ=-0.0091

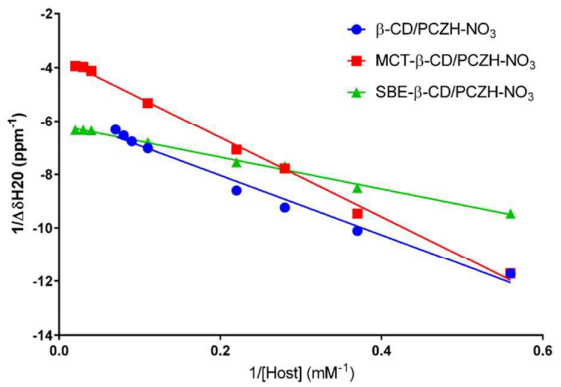

Figure 5. Ilustration of the Benesi-Hildebrand data treatment.

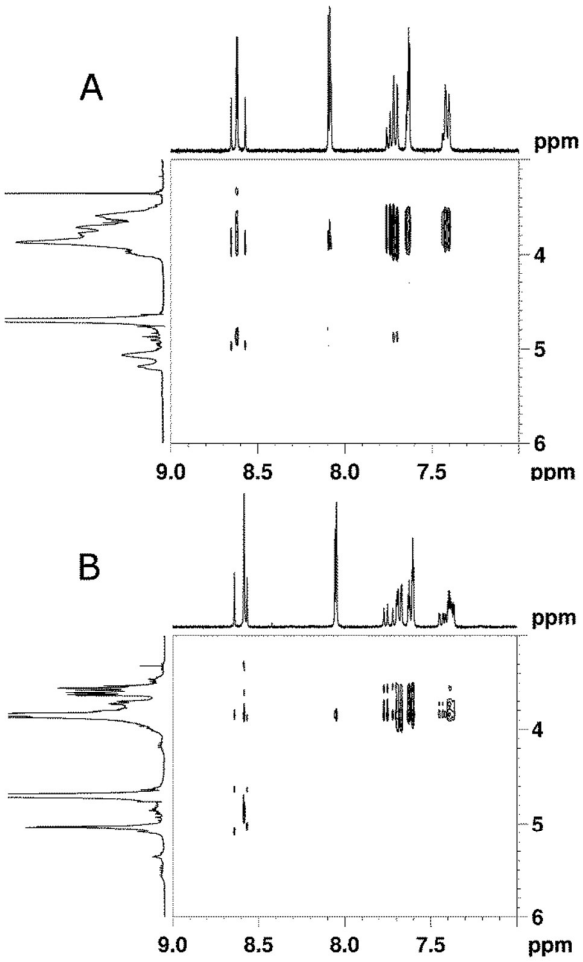

Figure 6. Expansions of ROESY spectra of **[A]** SBE7-β-CD/PCZH-NO_3 and **[B]** MCT-β-CD/PCZH-NO_3 inclusion complexes, recorded in phosphate buffered D_2O.

The ROESY spectra of MCT-β-CD/PCZH-NO_3 and SBE7-β-CD/PCZH-NO_3 inclusion complexes (Fig. 6) showed intramolecular NOE cross-peaks for H-3, H-5, H-17, H-19 and H-20 of PCZH-NO_3 protons and of the internal CD protons. These protons belong to the triazole (H-3 and H-5) and 2,4-diclorophenyl (H-17, H-19 and H-20) rings. Thus, it might be concluded that two types of inclusion complexes simultaneously exist in the solution: a first type, when the 2,4-diclorophenyl ring enters into the CD cavities, giving NOE cross peaks with protons H-17, H-19 and H-20, and a second type, when the triazole ring is inside the CD cavities, giving NOE cross-peaks with protons H-3 and H-5.

However, in the case of the triazole ring protons, their chemical shifts cannot be confidently attributed to the formation of an inclusion complex due to their sensitivity to many other physical and chemical parameters, such as solvent, pH, concentration, purity, temperature, etc. [44,45]. These additional factors can contribute to the larger variations of the chemical shifts obtained for the triazole ring compared with those of the 2,4-dichlorophenyl and can explains why, in this particular case, the modifications in the ^{1}H-NMR signals of the triazole ring are not totally related to the propiconazole interaction with cyclodextrins. Moreover, it is not possible to detect from which side of the cyclodextrin the inclusions occur.

The 2D ROESY spectrum for β-CD-SNa/PCZH-NO_3 was not conclusive, possibly because the $-SO_3^-$ radicals are directly linked to the hydroxylic oxygen of the cyclodextrin.

In silico computational studies

Docking simulations. Comparative docking and molecular dynamics simulations for PCZH-NO_3 in the presence of β-CD (as a model) and SBE7-β-CD were performed (Fig. 7). The 200 complexes generated by the docking algorithm in each case were clustered based on binding energy criteria and root mean square deviation of their conformation. In the case of β-CD with PCZH-NO_3, two types of clusters were obtained (Fig. 7A and 7B), when the propyl or dichlorophenyl radicals of PCZH-NO_3 entered through the secondary rim of β-CD. In the first case (Fig. 7A), the estimated binding free energy for the best pose in this cluster was -4.35 kcal/mol, which corresponds to a K_a of 1751 M^{-1} and is the same order of magnitude as the experimentally determined value by NMR titration (510 M^{-1}, ΔG = -3.64 kcal/mol). It should be noted that, due to propyl size, the PCZH-NO_3 dioxolanyl cycle was located inside the CD ring, near its glycoside residues, and that the 1,2,4-triazolylmethyl moiety of PCZH-NO_3 participates, through its NH+ group, in a hydrogen bond with a CD glycosidic oxygen. In the second case (Fig. 7B), the same hydrogen bond occurs with the 1,2,4-triazolylmethyl moiety, but the dioxolanyl ring sit is more exposed to the solvent, in a parallel plane with the secondary rim of CD, which also favoured hydrogen bond formation. The binding free energy was of -4.28 kcal/mol and the K_a of 1553 M^{-1}. These two clusters represent different modes of complexation with close binding free energies (and, consequently, close K_a values) which may coexist in solution.

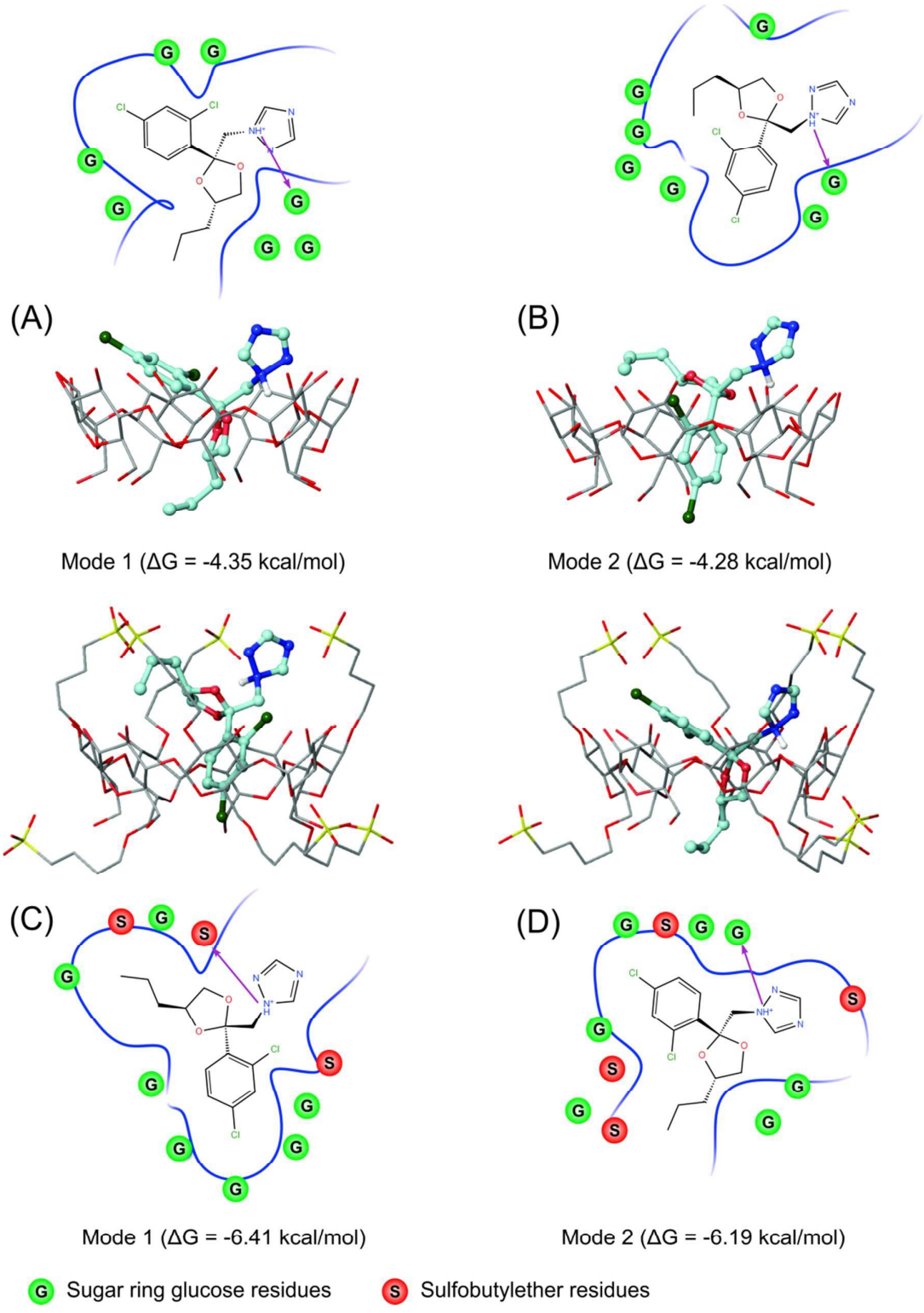

Figure 7. Conformations of inclusion complexes of **[A, B]** β-CD/PCZH-NO_3 and **[C, D]** SBE7-β-CD/PCZH-NO_3 obtained by docking simulations. The 2D diagrams of each complex emphasize the interactions of different groups of PCZH-NO_3 with pyranose and/or sulfobutylether residues. Arrows indicate hydrogen bonds between PCZH-NO_3 and CD.

Docking results for the SBE7-β-CD/PCZH-NO_3 complexes showed a different situation of the inclusion process from an energetic and conformational point of view (Fig. 7C – Mode 1 and Fig. 7D – Mode 2). In this case, the results provided high binding affinities [46,47] to the host molecules with binding free energies below -6.0 kcal/mol. The cluster with the highest affinity shows a conformation with the aromatic ring of the dichlorophenyl moiety embedded in the SBE7-β-CD cavity at the sugar ring level (Fig. 7C – Mode 1). Compared with the same inclusion mode into the non-substituted β-CD (Fig. 7B) the aromatic ring lies in a more elevated position towards the secondary rim of CD which allows a better interaction of the PCZH-NO_3 propyl group with the hydrophobic butyl arm of SBE7-β-CD. Moreover, a hydrogen bond occurred between the triazolylmethyl moiety of PCZH-NO_3 and the $-SO_3^-$ groups of the secondary rim of SBE7-β-CD. All these interactions increased binding free energy absolute value (-6.41 kcal/mol) and enhanced the binding affinity (to a K_a of 60144 M^{-1}) of SBE7-β-CD to PCZH-NO_3 compared to those of β-CD/PCZH-NO_3 complexes. Similar results (ΔG = -6.19 kcal/mol, K_a = 41225 M^{-1}) with those of Mode 1 were obtained when the supplementary interactions between the dichlorophenyl and propyl groups of PCZH-NO_3 and the hydrophobic butyl of SBE7-β-CD primary ring were considered (Mode 2). This explains the changes in the H3, H5, H17, H19 and H20 signals of PCZH-NO_3 seen in NMR (Fig. 2-4, Table 1) for the SBE7-β-CD/PCZH-NO_3 inclusion complex.

Both theoretically calculated and experimentally NMR titration measured K_a values display a consensus view of the PCZH-NO_3 complexation with higher affinity of the guest molecule for SBE7-β-CD (NMR K_a of 1050 M^{-1}) compared to β-CD (NMR K_a of 510 M^{-1}). Still, the calculated binding free energies are higher in absolute value than the experimental ones. A direct comparison in absolute values between theoretical and experimental association constants, however, should be regarded with care due to a couple of reasons. First, the free energy scoring function used by AutoDock 4.2 was trained to reproduce the binding constants in water while the NMR titration curves were obtained in water/DMSO (90/10) mixtures; the added co-solvents are known to be able to displace guest molecules from CD cavity even in low concentrations [48,49] while DMSO forms stable complexes with β-CD [50]. On the other hand the accuracy of the docking method should be considered when comparing theoretical predicted affinities to experimental ones; AutoDock 4.2 accuracy allows only for discrimination between milli-, micro- and nano-molar dissociation constants [51].

Molecular dynamics simulations. In docking experiments the substituted CD was considered a rigid entity, especially when assessing the optimum geometries of the complex. This is a major drawback of the method due to the fact that β-CDs are highly flexible molecules, especially when substituted. In this context, molecular dynamics simulations generate statistical ensembles of structures, which are a better approximate for the real guest-host structures. Moreover, the implicit representation of the solvent (as a continuum dielectric) may minimize the competing interactions of the guest molecule with the solvent molecules. Thus the explicit representation of the water molecules in the molecular dynamics simulations may provide further insights into the inclusion mechanism and stabilizing interactions [52].

Representative complexes with the highest AutoDock binding constant for both β-CD and SBE7-β-CD with PCZH-NO_3 were further evaluated by explicit solvent molecular dynamics simulations. On the most favourable inclusion modes, as suggested by the docking studies, four molecular dynamics simulations, two for each of β-CD and SBE7-β-CD in the presence of PCZH-NO_3, were performed. Complexes presented in Fig. 7 were solvated in water and, in the case of SBE7-β-CD/PCZH-NO_3, a necessary number of Na+ ions were added to assure overall neutrality of the system.

All complexes showed a good stability on the simulation time scale (50 ns) followed by monitoring the distances between the centres of mass of PCZH-NO_3 and the CD ring (see Fig. SI-1 in ESI: distances between COM of CD and PCZH-NO_3). Representative conformations for the inclusion complexes during the simulations were depicted in Fig. SI-2 (in ESI). A visual inspection of the trajectories showed that, in both β-CD/PCZH-NO_3 inclusion modes (i.e. with the propyl and the dichlorophenyl ring in the β-CD, respectively), the triazolylmethyl group adopts an orientation different from that suggested by docking simulations. The $-NH^+$ moiety becomes more solvent exposed, showing a steady preference for hydrogen bonding with water molecules (Fig. 8). Hydrogen bonding with the glycosidic oxygen or the CD hydroxyls, from C2 or C3, displayed reduced propensity. In the SBE7-β-CD/PCZH-NO_3 complexes this preference is preserved and accompanied by the formation of a persistent intermolecular hydrogen bond between the triazolylmethyl and the sulfate radical, in a similar way to Mode 1, as predicted by docking studies (Fig. 7C).

DSC studies

DSC is a useful tool in establishing the occurrence of host-guest interactions in solid state. After inclusion in the host molecule cavity, the melting profile of the guest molecule either reduces in intensity or completely disappears, with the possibility of simultaneous displacement [53]. As indicated in Fig 9A, the PCZH-NO_3 molecule exhibits a double peaked melting profile with temperature values at 128°C and 139°C. In a previous paper, our research group showed that this aspect is due to the presence of one minor and one major isomer of the guest molecule [10].

The double peaked intense melting profile of PCZH-NO_3 also appears for all physical mixtures (PM). The analysis of the DSC curves of the β-CD-SNa/PCZH-NO_3 (Fig. 9A), MCT-β-CD/PCZH-NO_3 (Fig. 9B) and SBE7-β-CD/PCZH-NO_3 (Fig. 9C) inclusion complexes showed that the two melting peaks of the guest molecule coalesce into a single and significantly reduced peak.

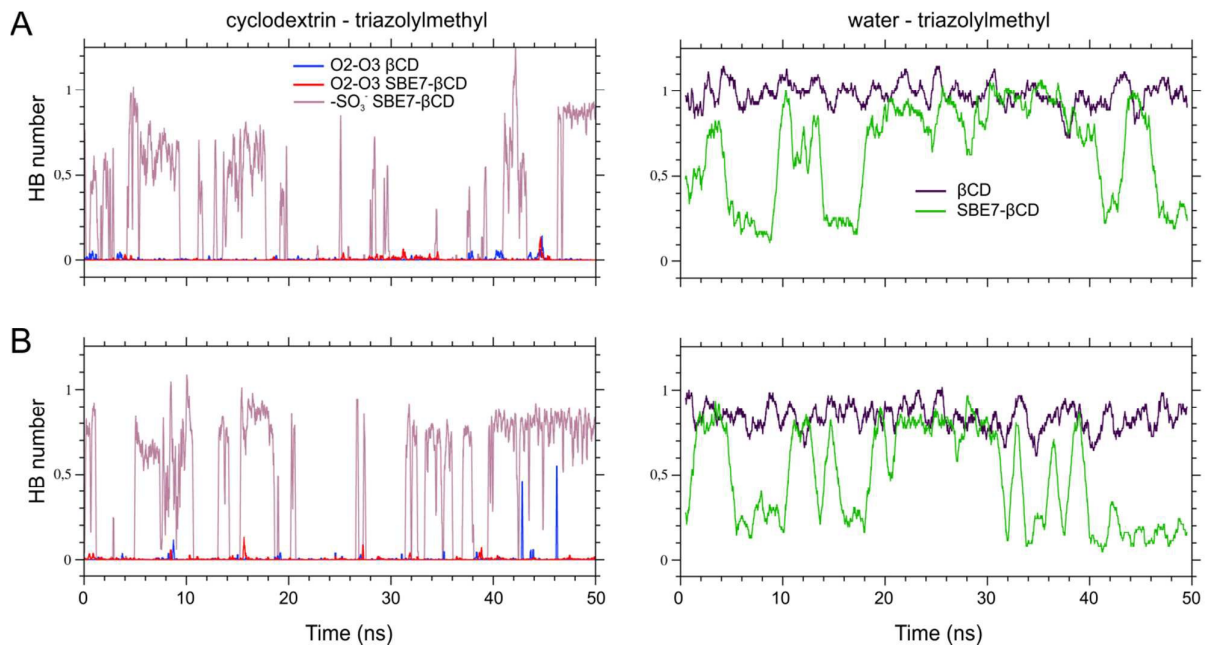

Figure 8. Number of hydrogen bonds (HB) between the triazolylmethyl group of PCZH-NO_3 and oxygens from C2 or C3 and the -SO_3^- group of sulfobutylether substituents of SBE7-β-CD: **[A]** PCZH-NO_3 dichlorophenyl group included in the CD cavity; **[B]** PCZH-NO_3 propyl group included in the CD cavity.

This peak is displaced towards seemingly lower temperatures (Tm = 133°C for β-CD-SNa/PCZH-NO_3 and Tm = 120°C for MCT-β-CD/PCZH-NO_3) and completely disappears for SBE7-β-CD/PCZH-NO_3, which indicates the formation of a new solid phase, due to complexation [54].

Inclusion efficiency values close to 100 % (99.90 % SBE7-β-CD/PCZH-NO_3, 99.69 % MCT-β-CD/PCZH-NO_3 and 99.73 % β-CD-SNa/PCZH-NO_3) were obtained by applying the equation (2) below [55], where ΔH_{mc} represents the melting enthalpy of the inclusion complex and ΔH_{mg} that of uncomplexed pure guest.

$$\% \text{ Inclusion} = 100\,(1 - \Delta H_{mc}/\Delta H_{mg}) \qquad (2)$$

The broad endothermic peaks in the DSC curves of studied inclusion complexes correspond to loss of crystallized water molecules from cavities of cyclodextrins.

Dissolution studies

Dissolution studies are routine tests in the pharmaceutical industry to effectively assess *in vitro* and *in vivo* behaviour of tested compounds. The dissolution rate profiles of inclusion compounds compared to the pure drug were represented graphically by plotting cumulative amount of PCZH-NO_3 dissolved vs. time (minutes).

In our case, the dissolution studies in water solutions of pH=6.8 showed an improved dissolution rate of PCZH-NO_3 in inclusion complexes compared to the free drug, in the following order: β-CD-SNa/PCZH-NO_3 > MCT-β-CD/PCZH-NO_3 > SBE7-β-CD/PCZH-NO_3 > β-CD/PCZH-NO_3 >> PCZH-NO_3 (Fig. 10).

Biological tests

The geometric means of the MIC values are presented in Table 2. All four complexes showed antifungal activity at low concentrations similar to those usually exhibited by voriconazole. There were no statistically significant differences between the complexes. The IC_{50} values shown in Table 3 were two to three orders of magnitude higher than the concentrations required for antifungal activity. The 95% CIs presented in the same table and the nonlinear fit of the curves shown in Fig. 11 indicate a significantly higher cytotoxicity for the complex with the parental β-CD compared to those with the other three CD derivatives.

The much lower concentrations required for the antifungal effect, compared to the IC_{50} cytotoxicity values, prove a high selectivity of the active compound for the fungal cells. The lack of significant differences in the antifungal susceptibility tests and the differences in cytotoxicity between the β-CD complex and the other three suggest that, in the case of PCZH-NO_3, the type of cyclodextrin may be more important for the interaction with the human organism than it is for the actual antifungal activity. In the case of other antifungal agents, however, significant improvements of their *in vitro* antifungal activity as a result of complexation have been reported [56–58].

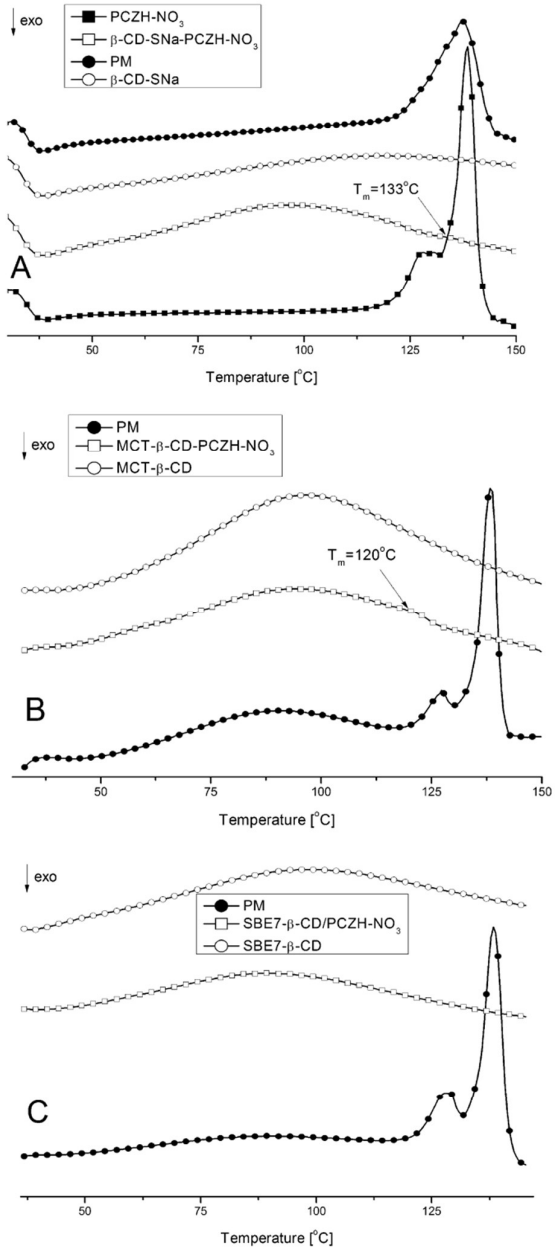

Figure 9. DSC heating curves of: **[A]** PCZH-NO_3, β-CD-SNa/PCZH-NO_3, physical mixture (PM) of β-CD-SNa and PCZH-NO_3, β-CD-SNa; **[B]** MCT-β-CD/PCZH-NO_3, MCT-β-CD, physical mixture of MCT-β-CD and PCZH-NO_3; **[C]** SBE7-β-CD/PCZH-NO_3, SBE7-β-CD and physical mixture of SBE7-β-CD and PCZH-NO_3.

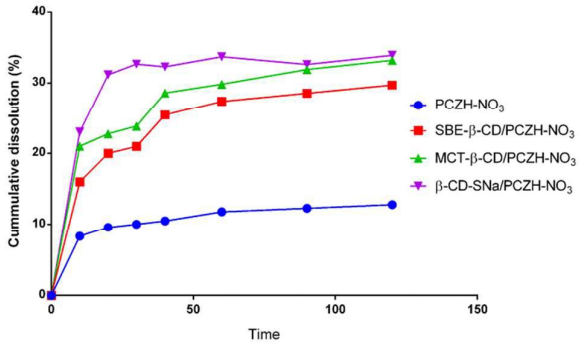

Figure 10. The dissolution profile of **[A]** the free drug PCZH-NO_3 compared to the inclusion complexes - **[B]** SBE7-β-CD/PCZH-NO_3, **[C]** MCT-β-CD/PCZH-NO_3 and **[D]** β-CD-SNa/PCZH-NO_3, at pH 6.8.

Table 2. Antifungal activities of the free PCZH-NO_3 and its inclusion complexes. The geometric means of the MIC values (mg/L).

Species	PCZH-NO_3	Inclusion complexes (cyclodextrin used)			
		β-CD	SBE7-β-CD	β-CD-SNa	MCT- β-CD
C. albicans	0.02	0.02	0.02	0.03	0.03
C. glabrata	0.04	0.04	0.05	0.05	0.08
Overall	0.03	0.03	0.03	0.04	0.05

Table 3. Cytotoxicity of the free PCZH-NO_3 and its inclusion complexes.

Compound	IC_{50} (mg/L)	95% CI (mg/L)
PCZH-NO_3	128	26 - 638
Inclusion complexes of PCZH-NO_3 (cyclodextrin used)		
β-CD	80	70 - 90
SBE7-β-CD	220	180 - 260
β-CD-SNa	240	210 - 280
MCT-β-CD	230	210 - 250

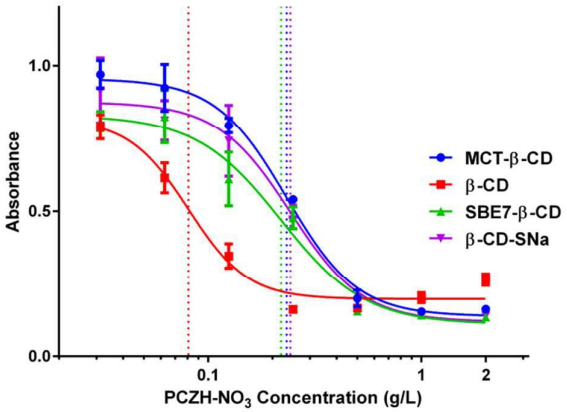

Figure 11. Cytotoxicity of the inclusion complexes of PCZH-NO_3 with β-CD and its derivatives - nonlinear fit of the dose response curves. The dotted lines indicate the IC_{50} values.

Conclusions

The ^{1}H- and 2D ROESY NMR studies demonstrated the formation of host-guest inclusion complexes between protonated propiconazole nitrate and three β-cyclodextrin derivatives, namely sulfobutylether-β-cyclodextrin, β-cyclodextrin-sulfated sodium salt and monochlorotriazinyl-β-cyclodextrin. Information offered by NMR was supported by *in silico* docking and molecular dynamics (with water as an explicit solvent) simulations.

Both theoretically calculated and experimentally NMR titration measured association constants values display a consensus view of the protonated propiconazole nitrate complexation with higher affinity of the guest molecule for sulfobutylether-β-cyclodextrin compared to β-cyclodextrin. This indicates a better complexation capacity for the modified cyclodextrin, which is due to additional stability induced by the interactions of the dioxolanyl and triazolic cycles with the glycosidic oxygens or the -SO_3^- groups of the cyclodextrin, depending on the complexation mode.

The inclusion of protonated propiconazole nitrate into the cyclodextrin cavity was also demonstrated through differential scanning calorimetry studies, which showed the formation of a new solid phase with different thermal properties compared to the physical mixtures of the two components.

An antifungal activity of monochlorotriazinyl-β-cyclodextrin alone could not be confirmed. The lower cytotoxicity of the inclusion complexes with the substituted cyclodextrins coupled with the lack of significant differences regarding the antifungal activity, compared to the complex with the parental β-cyclodextrin, suggests that the nature of the cyclodextrin is more relevant for the *in vivo* behaviour of the complexes rather than for the *in vitro* antifungal activity.

Acknowledgements

This publication benefited from the financial support of the project "Programme of excellency in the multidisciplinary doctoral and post-doctoral research of chronic diseases", contract no. POSDRU/159/1.5/S/133377, beneficiary "Gr. T. Popa" University of Medicine and Pharmacy of Iasi, project co-financed from the European Social Fund through the Sectoral Operational Programme Human Resources Development (SOP HRD) 2007-2013.

References

1 C. G. Pierce and J. L. Lopez-Ribot, *Expert Opin. Drug Discov.*, 2013, **8**, 1117–1126.
2 S. S. W. Wong, L. P. Samaranayake and C. J. Seneviratne, *Drug Discov. Today*, 2014, **19**, 1721–1730.
3 P. V. Sanitá, E. G. de Oliveira Mima, A. C. Pavarina, J. H. Jorge, A. L. Machado and C. E. Vergani, *Oral Surg. Oral Med. Oral Pathol. Oral Radiol.*, 2013, **116**, 562–569.
4 M. Weig and A. J. P. Brown, *Trends Microbiol.*, 2007, **15**, 310–317.
5 D. Maubon, C. Garnaud, T. Calandra, D. Sanglard and M. Cornet, *Intensive Care Med.*, 2014, **40**, 1241–1255.
6 M. Iman and A. Davood, *Med. Chem. Res.*, 2013, **23**, 2890–2899.
7 F. C. Odds, A. J. P. Brown and N. A. R. Gow, *Trends Microbiol.*, 2003, **11**, 272–279.
8 H. V. Bossche and L. Koymans, *Mycoses*, 1998, **41**, 32–38.
9 B. Minea, V. Nastasa, R. F. Moraru, A. Kolecka, M. M. Flonta, I. Marincu, A. Man, F. Toma, M. Lupse, B. Doroftei, N. Marangoci, M. Pinteala, T. Boekhout and M. Mares, *Eur. J. Clin. Microbiol. Infect. Dis.*, 2015, **34**, 367–383.
10 N. Marangoci, M. Mares, M. Silion, A. Fifere, C. Varganici, A. Nicolescu, C. Deleanu, A. Coroaba, M. Pinteala and B. C. Simionescu, *Results Pharma Sci.*, 2011, **1**, 27–37.
11 A. Fifere, N. Marangoci, S. Maier, A. Coroaba, D. Maftei and M. Pinteala, *Beilstein J. Org. Chem.*, 2012, **8**, 2191–2201.
12 S. V. Kurkov and T. Loftsson, *Int. J. Pharm.*, 2013, **453**, 167–180.
13 T. Loftsson and M. E. Brewster, *J. Pharm. Pharmacol.*, 2010, **62**, 1607–1621.
14 M. Vecsernyés, F. Fenyvesi, I. Bácskay, M. A. Deli, L. Szente and É. Fenyvesi, *Arch. Med. Res.*, 2014, **45**, 711–729.
15 M. Fukuda, D. A. Miller, N. A. Peppas and J. W. McGinity, *Int. J. Pharm.*, 2008, **350**, 188–196.
16 S. Gopinathan, E. O'Neill, L. A. Rodriguez, R. Champ, M. Phillips, A. Nouraldeen, M. Wendt, A. G. E. Wilson and J. A. Kramer, *J. Pharmacol. Toxicol. Methods*, 2013, **68**, 284–295.
17 L. García-Río, M. Méndez, M. R. Paleo and F. J. Sardina, *J. Phys. Chem. B*, 2007, **111**, 12756–12764.
18 K. Uekama, F. Hirayama and T. Irie, *Chem. Rev.*, 1998, **98**, 2045–2076.
19 Q. Yao, B. You, S. Zhou, M. Chen, Y. Wang and W. Li, *Spectrochim. Acta. A. Mol. Biomol. Spectrosc.*, 2014, **117**, 576–586.
20 H. Reuscher and R. Hirsenkorn, *J. Incl. Phenom. Mol. Recognit. Chem.*, 1996, **25**, 191–196.
21 V. Nardello-Rataj and L. Leclercq, *Beilstein J. Org. Chem.*, 2014, **10**, 2603–2622.
22 D. Vialaton, J. F. Pilichowski, D. Baglio, A. Paya-Perez, B. Larsen and C. Richard, *J. Agric. Food Chem.*, 2001, **49**, 5377–5382.
23 G. M. Morris, R. Huey, W. Lindstrom, M. F. Sanner, R. K. Belew, D. S. Goodsell and A. J. Olson, *J. Comput. Chem.*, 2009, **30**, 2785–2791.
24 M. W. Schmidt, K. K. Baldridge, J. A. Boatz, S. T. Elbert, M. S. Gordon, J. H. Jensen, S. Koseki, N. Matsunaga, K. A. Nguyen, S. Su, T. L. Windus, M. Dupuis and J. A. Montgomery, *J. Comput. Chem.*, 1993, **14**, 1347–1363.
25 E. Vanquelef, S. Simon, G. Marquant, E. Garcia, G. Klimerak, J. C. Delepine, P. Cieplak and F.-Y. Dupradeau, *Nucleic Acids Res.*, 2011, **39**, W511–517.
26 C. I. Bayly, P. Cieplak, W. Cornell and P. A. Kollman, *J. Phys. Chem.*, 1993, **97**, 10269–10280.
27 J. Wang, R. M. Wolf, J. W. Caldwell, P. A. Kollman and D. A. Case, *J. Comput. Chem.*, 2004, **25**, 1157–1174.
28 C. Cézard, X. Trivelli, F. Aubry, F. Djedaïni-Pilard and F.-Y. Dupradeau, *Phys. Chem. Chem. Phys. PCCP*, 2011, **13**, 15103–15121.
29 K. N. Kirschner and R. J. Woods, *Proc. Natl. Acad. Sci.*, 2001, **98**, 10541–10545.
30 K. N. Kirschner, A. B. Yongye, S. M. Tschampel, J. González-Outeiriño, C. R. Daniels, B. L. Foley and R. J. Woods, *J. Comput. Chem.*, 2008, **29**, 622–655.
31 G. M. Morris, D. S. Goodsell, R. S. Halliday, R. Huey, W. E. Hart, R. K. Belew and A. J. Olson, *J. Comput. Chem.*, 1998, **19**, 1639–1662.
32 A. S. Jain, A. A. Date, R. R. S. Pissurlenkar, E. C. Coutinho and M. S. Nagarsenker, *AAPS PharmSciTech*, 2011, **12**, 1163–1175.

33 W. L. Jorgensen, J. Chandrasekhar, J. D. Madura, R. W. Impey and M. L. Klein, *J. Chem. Phys.*, 1983, **79**, 926–935.
34 M. Parrinello and A. Rahman, *J. Appl. Phys.*, 1981, **52**, 7182–7190.
35 S. Nosé, *J. Chem. Phys.*, 1984, **81**, 511–519.
36 null Hoover, *Phys. Rev. A*, 1985, **31**, 1695–1697.
37 T. Darden, D. York and L. Pedersen, *J. Chem. Phys.*, 1993, **98**, 10089–10092.
38 S. Pronk, S. Páll, R. Schulz, P. Larsson, P. Bjelkmar, R. Apostolov, M. R. Shirts, J. C. Smith, P. M. Kasson, D. van der Spoel, B. Hess and E. Lindahl, *Bioinforma. Oxf. Engl.*, 2013, **29**, 845–854.
39 European Directorate for the quality of Medicines & HealthCare, *European Pharmacopoeia*, 8th edn., 2014.
40 M. C. Arendrup, M. Cuenca-Estrella, C. Lass-Flörl, W. Hope and T. Eucast-Afst, *Clin. Microbiol. Infect.*, 2012, **18**, E246–E247.
41 Promega Corporation, 2012.
42 L. Fielding, *Tetrahedron*, 2000, **56**, 6151–6170.
43 S. M. Ali, F. Asmat and M. Koketsu, *J. Incl. Phenom. Macrocycl. Chem.*, 2007, **59**, 191–196.
44 Teresa M.V.D. Pinho e Melo and Antonio M. d' A. Rocha Gonsalves, *Recent Research Developments in Heterocyclic Chemistry*, Research Signpost, 2007.
45 M. L. Roumestant, P. Viallefont, J. Elguero and R. Jacquier, *Tetrahedron Lett.*, 1969, **10**, 495–498.
46 S. Shityakov and C. Förster, *Adv. Appl. Bioinforma. Chem. AABC*, 2014, **7**, 23–36.
47 S. Shityakov, J. Broscheit and C. Förster, *Int. J. Nanomedicine*, 2012, **7**, 3211–3219.
48 Y. Liu, Y. Song, Y. Chen, Z.-X. Yang and F. Ding, *J. Phys. Chem. B*, 2005, **109**, 10717–10726.
49 H. Zhang, C. Ge, D. van der Spoel, W. Feng and T. Tan, *J. Phys. Chem. B*, 2012, **116**, 3880–3889.
50 T. Aree and N. Chaichit, *Carbohydr. Res.*, 2002, **337**, 2487–2494.
51 R. Huey, G. M. Morris, A. J. Olson and D. S. Goodsell, *J. Comput. Chem.*, 2007, **28**, 1145–1152.
52 A. Neamtu, N. Marangoci and V. Harabagiu, *Rev. Chim.*, 2013, **64**, 502–508.
53 A. Corciova, C. Ciobanu, A. Poiata, C. Mircea, A. Nicolescu, M. Drobota, C.-D. Varganici, T. Pinteala and N. Marangoci, *J. Incl. Phenom. Macrocycl. Chem.*, 2014, **81**, 71–84.
54 A. Corciova, C. Ciobanu, A. Poiata, A. Nicolescu, M. Drobota, C. D. Varganici, T. Pinteala, A. Fifere, N. Marangoci and C. Mircea, *Dig. J. Nanomater. Biostructures*, 2014, **9**, 1623–1637.
55 H. E. Grandelli, B. Stickle, A. Whittington and E. Kiran, *J. Incl. Phenom. Macrocycl. Chem.*, 2012, **77**, 269–277.
56 X.-L. Zhu, H.-B. Wang, Q. Chen, W.-C. Yang and G.-F. Yang, *J. Agric. Food Chem.*, 2007, **55**, 3535–3539.
57 G.-F. Yang, H.-B. Wang, W.-C. Yang, D. Gao and C.-G. Zhan, *J. Chem. Phys.*, 2006, **125**, 111104.
58 G.-F. Yang, H.-B. Wang, W.-C. Yang, D. Gao and C.-G. Zhan, *J. Phys. Chem. B*, 2006, **110**, 7044–7048.

TEXT

Inclusion complexes with sulfobutylether-β-cyclodextrin, β-cyclodextrin sulphated sodium salt and monochlorotriazinyl-β-cyclodextrin were characterized and assessed for antifungal activity and cytotoxicity.

GRAPHIC

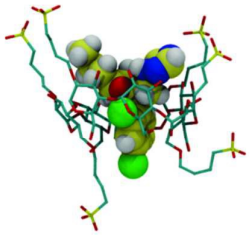

SBE-β-CD/PCZH-NO_3

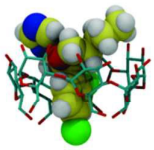

β-CD/PCZH-NO_3